ELSEVIER

Earth and Planetary Science Letters 181 (2000) 115–129

EPSL

www.elsevier.com/locate/epsl

# Hf–Nd isotopic evolution of the lower crust

Jeff D. Vervoort [a,*], P. Jonathan Patchett [a], Francis Albarède [b], Janne Blichert-Toft [b], Roberta Rudnick [c], Hilary Downes [d]

[a] *Department of Geosciences, University of Arizona, Tucson, AZ 85721, USA*
[b] *Ecole Normale Supérieure de Lyon, UMR CNRS 8515, 69364 Lyon Cedex 7, France*
[c] *Department of Earth and Planetary Sciences, Harvard University, 20 Oxford St., Cambridge, MA 02138, USA*
[d] *School of Earth Science, Birkbeck College, London WC1E 7HX, UK*

Received 22 November 1999; received in revised form 23 May 2000; accepted 25 May 2000

**Abstract**

We report Hf isotopic data for over 50 well studied lower crustal samples from three Proterozoic and Phanerozoic regions in southwest Europe, eastern Australia and southern Mexico. We use these data to characterize the Lu–Hf isotopic composition of the lower crust and, in combination with existing Sm–Nd data, to constrain coupled Hf–Nd isotopic behavior and evolution within this reservoir. Although most of these samples have present-day parent/daughter (p/d) ratios consistent with Hf–Nd evolution within the terrestrial Hf–Nd array, some samples have divergent p/d ratios that would evolve out of the terrestrial array in 1 Ga or less. The present-day $^{176}Hf/^{177}Hf$ and $^{143}Nd/^{144}Nd$ isotopic compositions of all samples, with one lone exception, plot within the terrestrial array. This indicates that (1) some present-day p/d ratios may be a relatively recently acquired characteristic through magmatic or metamorphic processes not related to the time-integrated Sm/Nd and Lu/Hf ratios of their sources, and/or (2) the Lu/Hf and Sm/Nd p/d variations exist on a small hand-size scale but not necessarily on a larger scale. The lower crust, from this initial data set, is broadly similar to the upper crust in terms of both its present-day p/d values and time-integrated Lu–Hf and Sm–Nd evolution. As a result, the lower crust appears to have a Hf and Nd isotopic composition similar to that of all other crust and mantle reservoirs so far characterized. 

*Keywords:* hafnium; isotope ratios; lower crust; isotope fractionation; composition; xenoliths; granulites

## 1. Introduction

Although the detailed nature of the lower crust is not well known, there are increasingly tighter constraints on its bulk chemical and isotopic composition from recent geochemical studies of xenoliths (e.g. [1] and references therein) and exposed granulite terranes (e.g. [2] and references therein), as well as P-T-t (e.g. [3–5]) and integrated geophysical studies [6–8]. This multidisciplinary work demonstrates that the lower crust is highly heterogeneous, generally in the granulite metamorphic grade, and is overall more mafic and depleted in incompatible and heat producing elements (HPE: e.g. K, U, Th) than the upper and middle crust [8]. The Hf isotopic composition and

* Corresponding author. Tel.: +1-520-626-9122; Fax: +1-520-621-2672; E-mail: vervoort@geo.arizona.edu

0012-821X/00/$ – see front matter 
PII: S0012-821X(00)00170-9

evolution of the lower crust, however, is not well constrained.

There are several fundamental reasons why we should be interested in the Hf isotopic composition of the lower crust and why constraining the isotopic composition of the lower crust is essential for our understanding of the Hf–Nd isotopic behavior in the bulk silicate Earth (BSE).

First, the lower crust is depleted in incompatible elements and HPE compared with the upper crust, suggesting the former has been reworked by melting and intracrustal differentiation. A mineral that may leave a distinctive fingerprint of this process is garnet, which occurs in basaltic [9] and pelitic [10] lower crustal lithologies. If garnet in these rocks is a purely metamorphic phase, then its formation will not produce significant bulk rock fractionation of Lu/Hf and Sm/Nd ratios. If, however, garnet is residual from melting or differentiation events, it will impart an elevated Lu/Hf ratio to the bulk rock due to the very high partition coefficients of garnet for Lu compared to Hf. Such high Lu/Hf ratios have been reported for two garnet–granulite xenoliths from Kilbourne Hole, New Mexico [11]. If such high Lu/Hf lithologies are typical of lower crust, then it will rapidly evolve toward highly radiogenic Hf isotopic compositions and should be recognizable in xenoliths and magmas that are derived from or interact with the lower crust.

Second, the overwhelming majority of mantle and upper crustal lithologies examined thus far lie along a single, well correlated $^{176}Hf/^{177}Hf$–$^{143}Nd/^{144}Nd$ isotopic array. This includes MORBs, OIBs, IAVs and continental crust of a wide range of lithologies, Archean to recent (data of many authors, see [12,13] for a compilation of sources and [14–18] for recent data). This indicates that, to a first approximation, Lu–Hf and Sm–Nd fractionate in a similar fashion in all terrestrial reservoirs. However, if the lower crust contains widespread residual or cumulate garnet, it might develop 'decoupled' Hf–Nd isotopic compositions that will evolve out of the terrestrial Hf–Nd array.

Third, an outstanding problem with respect to the Hf–Nd isotopic systematics of the silicate Earth is that the terrestrial Hf–Nd array appears to lie significantly above the BSE composition based on the chondritic Sm–Nd and Lu–Hf values currently in use [19–21]. If the chondritic Hf–Nd values accurately represent BSE Hf–Nd isotopic compositions, then the BSE composition should lie along a mixing hyperbola between bulk crust and depleted mantle [21]. It has been suggested [21], however, that the most plausible mixing hyperbolae pass above BSE and that this indicates the existence of a hidden reservoir to balance the terrestrial array with BSE. If the lower crust is characterized by high time-integrated Lu/Hf ratios and hence anomalously radiogenic Hf isotopic compositions, the problem is exacerbated because the bulk crust will plot even further above the terrestrial array.

In this paper, we characterize the Hf isotopic composition of the lower crust and, in conjunction with published Sm–Nd isotopic data, examine coupled Hf–Nd behavior and evolution in this relatively inaccessible region. We report Hf isotope data for several suites of lower crustal samples that have been thoroughly characterized by previous geochemical, petrological and isotopic studies (references below). These include: xenoliths from Mesozoic to recent volcanic rocks in the Massif Central (France) and the Iberian belt (Spain); xenoliths within the McBride and Chudleigh volcanic provinces in north Queensland, Australia; and xenoliths and exposed Proterozoic granulite and eclogite terranes in southern Mexico. The geological setting of each of these suites has been described in detail elsewhere (see below) but brief geological summaries are given below to provide background for the data presented herein.

## 2. Geological overview of analyzed samples

### 2.1. Massif Central, France

The lower crustal xenoliths we analyzed from the Massif Central occur in Neogene (ca. 4–7 Ma old) volcanic conduits or breccia 'pipes' from Bournac and Roche Pointue in France [22]. These volcanic conduits cut through late Paleozoic granites and Hercynian gneisses [22,23] and contain

xenoliths that are well characterized (e.g. [22–26]). Zircon ages for the Massif Central xenoliths are approximately 300 Ma [27] and it is thought that the mafic granulites were produced during a Hercynian underplating event that caused the pre-existing metasedimentary crust to melt and form the abundant granites exposed in the Massif Central [28]. We analyzed metaigneous (mafic and intermediate-felsic) and metasedimentary xenoliths from both localities. All the Massif Central xenoliths contain garnet with the exception of three mafic metaigneous samples (Table 1). The geochemistry (including Nd and Sr isotopes) of the Massif Central xenoliths analyzed for Hf isotopes in this paper has been previously described in [23].

### 2.2. Spanish central system

The xenoliths from the Hercynian central region of Spain [29] occur in an Early to Middle Jurassic alkaline dike swarm [30]. These dikes intrude Hercynian (ca. 300 Ma [27,31]) granites and Late Proterozoic to Paleozoic metamorphic rocks [29] and carry xenoliths of mainly felsic metaigneous compositions ($\sim$95%) and rare mafic metaigneous and metapelitic compositions. Thermobarometric calculations on mineral assemblages in these samples [29] indicate lower crustal equilibration conditions ($\sim$850°–950°C, 7–11 kbar). We analyzed six felsic metaigneous xenoliths from two locations (La Paramera and Peguerinos) in the Spanish central system [31], all of which contain garnet as a major phase [29]. Villaseca et al. [29] concluded that the felsic granulite xenoliths represent restites following extraction of a granitic melt similar in composition to the Hercynian granites [31]. Major element and trace element as well as Nd and Sr isotopic data for the samples we analyzed are reported in [29].

### 2.3. McBride and Chudleigh volcanic provinces, Queensland, Australia

The xenoliths from northeast Australia are hosted by basalts in two Pliocene–Pleistocene ($<3$ Ma) volcanic provinces in north Queensland [32]. The basalts from both provinces were erupted through diverse rock types ranging from the Proterozoic granites and metamorphic rocks of the Georgetown Inlier [33] to Paleozoic volcanic, plutonic and sedimentary rocks of the Tasman fold belt [34].

Xenoliths from the McBride Province are predominantly mafic, but a significant number (20–30%) of felsic to intermediate compositions also occur [35]. The latter are mostly metaigneous with lesser amounts of metapelites. All McBride xenoliths underwent high-grade metamorphism about 300–200 Ma ago and the protoliths for many of the xenoliths are Permo–Triassic in age, with the exception of a few xenoliths with Proterozoic crystallization ages ($\sim$1.5 Ga) as indicated by U–Pb ages of zircons [36]. These later ages correspond approximately to the age of the Georgetown Inlier, which was overprinted by the widespread Permo–Triassic metamorphic orogenic event. We analyzed eight mafic metaigneous and three metasedimentary/felsic metaigneous xenoliths from the McBride suite, all but two of which are garnet-bearing.

Xenoliths from the Chudleigh volcanic province are exclusively mafic in composition [34]. The xenoliths have been interpreted to be young (Cenozoic) cumulates formed from a mafic magma evolving by fractional crystallization and assimilation of deep crustal rocks [34,37], which crystallized at mid to lower crustal levels [38,39]. We analyzed 11 mafic xenoliths from the Chudleigh volcanic province, four of which are garnet-bearing.

Major and trace element, Nd, Sr, Pb, O and Os isotopic data for McBride and Chudleigh are reported in [34,35,37,40–42]. These xenolith suites thus represent the most completely characterized samples of lower crust currently described in the literature.

### 2.4. Mexican lower crustal granulites

Samples of the lower crust of Mexico exist as both tectonic slivers exposed throughout the Mexican Cordillera [43] and as xenoliths carried in recent volcanic rocks [44]. We analyzed three Mexican lower crustal granulites. Two of these are garnet-bearing metapelites from exposures in

Table 1
Hf and Nd isotopic data

| Sample | Gt? | $^{176}Hf/^{177}Hf$ | $^{176}Lu/^{177}Hf$ | $^{143}Nd/^{144}Nd$ | $\frac{^{147}Sm}{^{144}Nd}$ | Concentrations | | | | $\varepsilon_{Hf(0)}$ | $\varepsilon_{Nd(0)}$ | $t_{Hf-DM}$ | $t_{Nd-DM}$ | $f_{Lu/Hf}$ | $f_{Sm/Nd}$ | $F$ | Nd data source |
|---|---|---|---|---|---|---|---|---|---|---|---|---|---|---|---|---|---|
| | | | | | | Lu | Hf | Sm | Nd | | | | | | | | |
| **Massif Central** | | | | | | | | | | | | | | | | | |
| *Mafic metaigneous* | | | | | | | | | | | | | | | | | |
| H229A | | 0.282860 ± 5 | 0.0223 | 0.512511 ± 107 | 0.1521 | 0.32 | 2.01 | 3.45 | 13.75 | 3.11 | −2.48 | 1.18 | 1.58 | −0.33 | −0.23 | 1.46 | [19] |
| 17B1 | | 0.282716 ± 5 | 0.0183 | 0.512433 ± 20 | 0.1407 | 0.45 | 3.48 | 5.48 | 23.59 | −1.98 | −4.00 | 1.31 | 1.50 | −0.45 | −0.28 | 1.59 | [19] |
| RP-8 | Gt | 0.282799 ± 5 | 0.0286 | 0.512380 ± 22 | 0.1382 | 0.68 | 3.36 | 7.83 | 34.25 | 0.95 | −5.03 | 2.25 | 1.55 | −0.15 | −0.30 | 0.49 | [19] |
| RP-10 | Gt | 0.282502 ± 5 | 0.0184 | 0.512159 ± 12 | 0.1309 | 0.24 | 3.70 | 9.55 | 44.12 | −9.55 | −9.34 | 1.86 | 1.82 | −0.45 | −0.33 | 1.34 | [19] |
| RP-11 | | 0.282935 ± 11 | 0.0395 | 0.512611 ± 24 | 0.1683 | 0.26 | 0.94 | 2.29 | 8.23 | 5.76 | −0.53 | – | 1.81 | 0.18 | −0.14 | −1.27 | [19] |
| BOU-13 | Gt | 0.282501 ± 5 | 0.00332 | 0.512178 ± 21 | 0.1077 | 0.10 | 4.27 | 4.79 | 26.90 | −9.58 | −8.97 | 1.07 | 1.40 | −0.90 | −0.45 | 1.99 | [19] |
| *Felsic–intermediate metaigneous* | | | | | | | | | | | | | | | | | |
| BAL-715 | Gt | 0.282583 ± 8 | 0.0175 | | | 0.35 | 2.80 | | | −6.68 | | 1.59 | | −0.48 | | | |
| BAL-715.2 | Gt | 0.282536 ± 3 | 0.0104 | | | 0.33 | 4.53 | | | −8.35 | | 1.27 | | −0.69 | | | |
| BAL-1046 | Gt | 0.282518 ± 5 | 0.00750 | 0.512170 ± 20 | 0.1132 | 0.57 | 10.73 | 13.19 | 70.44 | −8.98 | −9.13 | 1.18 | 1.48 | −0.78 | −0.42 | 1.83 | [19] |
| *Metasediments* | | | | | | | | | | | | | | | | | |
| 830 | Gt | 0.282333 ± 5 | 0.00325 | 0.512048 ± 21 | 0.0894 | 0.25 | 10.82 | 10.10 | 68.31 | −15.52 | −11.51 | 1.31 | 1.35 | −0.90 | −0.55 | 1.66 | [19] |
| 831 | Gt | 0.282496 ± 5 | 0.0106 | 0.512137 ± 21 | 0.0934 | 0.51 | 6.78 | 7.31 | 47.67 | −9.76 | −9.77 | 1.35 | 1.28 | −0.68 | −0.53 | 1.30 | [19] |
| 8310 | Gt | 0.282434 ± 5 | 0.0134 | 0.512094 ± 45 | 0.1195 | 0.60 | 6.34 | 6.24 | 31.54 | −11.95 | −10.61 | 1.63 | 1.71 | −0.60 | −0.39 | 1.53 | [19] |
| 8330 | Gt | 0.282435 ± 4 | 0.0145 | 0.512038 ± 21 | 0.1210 | 0.62 | 6.02 | 8.15 | 40.72 | −11.92 | −11.70 | 1.71 | 1.82 | −0.56 | −0.39 | 1.47 | [19] |
| 8340 | Gt | 0.282488 ± 7 | 0.0129 | 0.512274 ± 33 | 0.1325 | 0.64 | 7.02 | 6.78 | 30.95 | −10.04 | −7.10 | 1.49 | 1.64 | −0.61 | −0.33 | 1.88 | [19] |
| 8320 | Gt | 0.282502 ± 9 | 0.0170 | 0.512215 ± 22 | 0.1257 | 0.41 | 3.44 | 4.31 | 20.76 | −9.55 | −8.25 | 1.74 | 1.62 | −0.49 | −0.36 | 1.36 | [19] |
| 17BA | Gt | 0.282502 ± 6 | 0.0239 | 0.512206 ± 26 | 0.1495 | 0.48 | 2.86 | 3.33 | 13.47 | −9.55 | −8.43 | 2.56 | 2.23 | −0.29 | −0.24 | 1.19 | [19] |
| **Spanish central system** | | | | | | | | | | | | | | | | | |
| *Felsic metaigneous* | | | | | | | | | | | | | | | | | |
| U-145 | Gt | 0.282636 ± 6 | 0.0165 | 0.512379 ± 8 | 0.1396 | 0.67 | 5.74 | 6.25 | 27.10 | −4.81 | −5.05 | 1.39 | 1.58 | −0.51 | −0.29 | 1.74 | [25] |
| U-146 | Gt | 0.282484 ± 5 | 0.0133 | 0.512167 ± 12 | 0.1113 | 0.58 | 6.21 | 4.07 | 22.10 | −10.18 | −9.19 | 1.52 | 1.46 | −0.60 | −0.43 | 1.39 | [25] |
| U-147 | Gt | 0.282447 ± 6 | 0.0175 | 0.512122 ± 5 | 0.1487 | 0.55 | 4.46 | 6.64 | 27.00 | −11.49 | −10.07 | 1.92 | 2.40 | −0.48 | −0.24 | 1.95 | [25] |
| U-152 | Gt | 0.282487 ± 6 | 0.0105 | 0.512217 ± 7 | 0.1307 | 0.58 | 7.77 | 8.13 | 37.60 | −10.08 | −8.21 | 1.37 | 1.71 | −0.68 | −0.34 | 2.04 | [25] |
| U-155 | Gt | 0.282594 ± 5 | 0.0166 | 0.512333 ± 4 | 0.1378 | 0.71 | 6.06 | 6.02 | 26.40 | −6.29 | −5.95 | 1.50 | 1.64 | −0.50 | −0.30 | 1.68 | [25] |
| U-157 | Gt | 0.282566 ± 5 | 0.0158 | 0.512248 ± 4 | 0.1335 | 0.65 | 5.83 | 6.14 | 27.80 | −7.29 | −7.61 | 1.50 | 1.71 | −0.53 | −0.32 | 1.64 | [25] |
| Mexican garnet-bearing pelites | | | | | | | | | | | | | | | | | |
| MOL-5-86 | Gt | 0.282159 ± 5 | 0.000823 | 0.511833 ± 9 | 0.1097 | 0.02 | 2.56 | 0.14 | 0.76 | −21.68 | −15.70 | 1.46 | 1.93 | −0.98 | −0.44 | 2.21 | [40] |
| OAX-5-86 | Gt | 0.282288 ± 4 | 0.0131 | 0.511962 ± 6 | 0.1102 | 0.79 | 8.59 | 6.51 | 35.71 | −17.12 | −13.19 | 1.90 | 1.75 | −0.61 | −0.44 | 1.38 | [40] |
| T-18-87 | Gt | 0.282652 ± 5 | 0.0261 | 0.512580 ± 6 | 0.1871 | 0.67 | 3.64 | 7.89 | 25.51 | −4.24 | −1.13 | 2.41 | 3.25 | −0.22 | −0.05 | 4.47 | [40] |
| Mexican garnet-bearing eclogites | | | | | | | | | | | | | | | | | |
| D-7814 | Gt | 0.282772 ± 6 | 0.00983 | 0.512797 ± 9 | 0.1521 | 0.32 | 4.57 | 6.25 | 24.84 | 0.00 | 3.10 | 0.82 | 0.88 | −0.71 | −0.23 | 3.11 | [0] |
| M-7 | Gt | 0.283154 ± 13 | 0.0390 | 0.513164 ± 11 | 0.2300 | 0.41 | 1.49 | 2.14 | 5.63 | 13.51 | 10.26 | – | 0.12 | 0.17 | 0.17 | 0.99 | [0] |
| MP-3 | Gt | 0.282775 ± 6 | 0.0102 | 0.512815 ± 16 | 0.1539 | 0.24 | 3.39 | 4.68 | 18.38 | 0.11 | 3.45 | 0.83 | 0.86 | −0.69 | −0.22 | 3.19 | [0] |
| MI-6 | Gt | 0.283194 ± 15 | 0.0402 | 0.513143 ± 8 | 0.2302 | 0.42 | 1.47 | 2.14 | 5.63 | 14.92 | 9.85 | – | – | 0.20 | 0.17 | 1.19 | [0] |

Table 1
Hf and Nd isotopic data

| Sample | Gt? | $^{176}Hf/^{177}Hf$ | $^{176}Lu/^{177}Hf$ | $^{143}Nd/^{144}Nd$ | $\frac{^{147}Sm}{^{144}Nd}$ | Concentrations | | | | $\varepsilon_{Hf(0)}$ | $\varepsilon_{Nd(0)}$ | $t_{Hf-DM}$ | $t_{Nd-DM}$ | $f_{Lu/Hf}$ | $f_{Sm/Nd}$ | $F$ | Nd data source |
|---|---|---|---|---|---|---|---|---|---|---|---|---|---|---|---|---|---|
| | | | | | | Lu | Hf | Sm | Nd | | | | | | | | |
| **Chudleigh volcanic province** | | | | | | | | | | | | | | | | | |
| *Mafic metaigneous* | | | | | | | | | | | | | | | | | |
| 83-107 | | 0.282916 ± 47 | 0.0404 | 0.512421 ± 16 | 0.1236 | 0.02 | 0.05 | 0.31 | 1.59 | 5.09 | −4.23 | – | 1.23 | 0.21 | −0.37 | −0.56 | [30] |
| 83-112 | | 0.282676 ± 10 | 0.00825 | 0.512598 ± 26 | 0.1627 | 0.13 | 2.15 | 1.66 | 6.17 | −3.39 | −0.78 | 0.94 | 1.65 | −0.75 | −0.17 | 4.36 | [30] |
| 83-112.2 | | 0.282629 ± 5 | 0.00789 | 0.512598 ± 26 | 0.1627 | 0.11 | 2.02 | 1.66 | 6.17 | −5.06 | −0.78 | 1.01 | 1.65 | −0.76 | −0.17 | 4.42 | [30] |
| 83-114 | Gt | 0.282757 ± 11 | 0.0244 | 0.512507 ± 18 | 0.1860 | 0.10 | 0.55 | 1.10 | 3.59 | −0.53 | −2.56 | 1.74 | 3.52 | −0.27 | −0.05 | 4.93 | [30] |
| 83-125 | Gt | 0.283024 ± 15 | 0.0301 | 0.512681 ± 20 | 0.1752 | 0.08 | 0.37 | 0.94 | 3.26 | 8.91 | 0.84 | 1.27 | 1.86 | −0.10 | −0.11 | 0.91 | [30] |
| 83-127 | | 0.283029 ± 16 | 0.0182 | 0.512638 ± 32 | 0.1201 | 0.02 | 0.14 | 0.30 | 1.53 | 9.09 | 0.00 | 0.50 | 0.84 | −0.46 | −0.39 | 1.17 | [30] |
| 83-131 | Gt | 0.282962 ± 18 | 0.0231 | 0.512594 ± 20 | 0.1645 | 0.05 | 0.33 | 0.62 | 2.26 | 6.72 | −0.86 | 0.89 | 1.72 | −0.31 | −0.16 | 1.89 | [30] |
| 83-140 | | 0.282812 ± 18 | 0.0255 | 0.512325 ± 32 | 0.1528 | 0.06 | 0.35 | 0.89 | 3.53 | 1.41 | −6.11 | 1.66 | 2.06 | −0.24 | −0.22 | 1.06 | [30] |
| 83-110 | | 0.283019 ± 10 | 0.0358 | 0.512916 ± 36 | 0.2541 | 0.27 | 1.06 | 1.73 | 4.13 | 8.73 | 5.42 | – | – | 0.07 | 0.29 | 0.25 | [30] |
| 83-115 | | 0.282997 ± 7 | 0.0330 | 0.512756 ± 14 | 0.2396 | 0.32 | 1.36 | 2.46 | 6.20 | 7.96 | 2.30 | 2.24 | – | −0.01 | 0.22 | −0.06 | [30] |
| 83-126 | | 0.282961 ± 8 | 0.0254 | 0.512693 ± 38 | 0.1823 | 0.12 | 0.65 | 1.66 | 5.52 | 6.68 | 1.07 | 1.06 | 2.21 | −0.24 | −0.07 | 3.25 | [30] |
| BC | Gt | 0.283208 ± 9 | 0.0302 | 0.513126 ± 36 | 0.2375 | 0.17 | 0.81 | 1.29 | 3.38 | 15.42 | 9.52 | 0.11 | – | −0.10 | 0.21 | −0.47 | [30] |
| **McBride volcanic province** | | | | | | | | | | | | | | | | | |
| *Mafic metaigneous* | | | | | | | | | | | | | | | | | |
| 83-158 | Gt | 0.283156 ± 9 | 0.0467 | 0.512885 ± 11 | 0.2304 | 0.55 | 1.67 | 3.10 | 8.13 | 13.58 | 4.82 | – | – | 0.40 | 0.17 | 2.32 | [32] |
| 85-106 | Gt | 0.283062 ± 6 | 0.0186 | 0.512964 ± 7 | 0.1954 | 0.29 | 2.21 | 3.62 | 11.20 | 10.26 | 6.36 | 0.43 | 1.55 | −0.44 | −0.01 | 67.10 | [32] |
| 85-100 | | 0.282421 ± 8 | 0.0121 | 0.511956 ± 4 | 0.1273 | 0.23 | 2.69 | 4.28 | 20.32 | −12.41 | −13.30 | 1.57 | 2.10 | −0.64 | −0.35 | 1.81 | [32] |
| 85-108 | Gt | 0.283036 ± 8 | 0.0358 | 0.512146 ± 4 | 0.1383 | 0.31 | 1.23 | 4.47 | 19.49 | 9.34 | −9.60 | 4.01 | 2.02 | 0.07 | −0.30 | −0.24 | [32] |
| 85-108.2 | Gt | 0.283034 ± 8 | 0.0346 | 0.512146 ± 4 | 0.1383 | 0.30 | 1.21 | 4.47 | 19.49 | 9.27 | −9.60 | 2.74 | 2.02 | 0.04 | −0.30 | −0.12 | [32] |
| 85-120 | | 0.282649 ± 6 | 0.0210 | 0.512196 ± 11 | 0.1529 | 0.27 | 1.83 | 3.95 | 15.61 | −4.35 | −8.62 | 1.72 | 2.38 | −0.37 | −0.22 | 1.66 | [32] |
| 83-159 | Gt | 0.282100 ± 7 | 0.00798 | 0.511887 ± 5 | 0.1370 | 0.46 | 8.10 | 4.31 | 19.02 | −23.76 | −14.65 | 1.90 | 2.50 | −0.76 | −0.30 | 2.51 | [32] |
| 85-107 | Gt | 0.282380 ± 5 | 0.00391 | 0.512011 ± 10 | 0.1370 | 0.52 | 19.01 | 5.73 | 21.49 | −13.86 | −12.23 | 1.26 | 2.26 | −0.88 | −0.30 | 2.91 | [32] |
| 85-114 | Gt | 0.282507 ± 5 | 0.0463 | 0.512430 ± 25 | 0.1880 | 0.89 | 2.72 | 1.81 | 5.82 | −9.37 | −4.06 | – | – | 0.39 | −0.04 | −8.76 | [32] |
| 85-114.2 | Gt | 0.282502 ± 5 | 0.0468 | 0.512430 ± 25 | 0.1880 | 0.91 | 2.75 | 1.81 | 5.82 | −9.55 | −4.06 | – | – | 0.40 | −0.04 | −9.06 | [32] |
| *Metasediments/felsic metaigneous* | | | | | | | | | | | | | | | | | |
| 83-157 | Gt | 0.282135 ± 9 | 0.0115 | 0.511724 ± 5 | 0.1319 | 1.30 | 7.69 | 6.00 | 27.50 | −22.53 | −17.83 | 2.08 | 2.64 | −0.66 | −0.33 | 1.99 | [32] |
| 83-160 | Gt | 0.282668 ± 7 | 0.0210 | 0.512280 ± 13 | 0.1265 | 0.62 | 4.20 | 5.11 | 24.40 | −3.68 | −6.98 | 1.65 | 1.52 | −0.37 | −0.36 | 1.04 | [32] |
| 83-162 | Gt | 0.282736 ± 9 | 0.0360 | 0.512285 ± 14 | 0.1887 | 1.25 | 4.91 | 5.86 | 18.80 | −1.27 | −6.89 | – | – | 0.08 | −0.04 | −1.93 | [32] |

Sm–Nd isotopic data published previously with the exception of Mexican garnet eclogites ([0], this study). 2σ errors for Hf concentrations are $<0.5\%$ and for Lu concentrations and $^{176}Lu/^{177}Hf$ are $<1.0\%$. $^{176}Hf/^{177}Hf$ ratios corrected for mass fractionation with $^{179}Hf/^{177}Hf = 0.7325$. For calculation of $\varepsilon_{Hf}$ values, we used $^{176}Hf/^{177}Hf_{CHUR(0)} = 0.282772$ and $^{176}Lu/^{177}Hf_{CHUR(0)} = 0.0332$. $\varepsilon_{Hf(0)}$, $\varepsilon_{Nd(0)}$ = present-day $\varepsilon$ Hf and Nd values. $f_{Lu/Hf} = [(^{176}Lu/^{177}Hf_{sample})/(^{176}Lu/^{177}Hf_{CHUR}) - 1]$; $f_{Sm/Nd}$ is analogous. $t_{Hf-DM} = (1/\lambda)\mathrm{Ln}[((^{176}Hf/^{177}Hf)_{sample} - (^{176}Hf/^{177}Hf)_{DM})/((^{176}Lu/^{177}Hf)_{sample} - (^{176}Lu/^{177}Hf)_{DM}) + 1]$; $t_{Nd-DM}$ is analogous. For calculation of $t_{Hf-DM}$ and $t_{Nd-DM}$, we used the following values for the present-day depleted mantle. $^{176}Hf/^{177}Hf = 0.283224$; $^{176}Lu/^{177}Hf = 0.03813$; $^{143}Nd/^{144}Nd = 0.513151$; $^{147}Sm/^{144}Nd = 0.2137$. 'Gt' signifies a garnet-bearing sample.

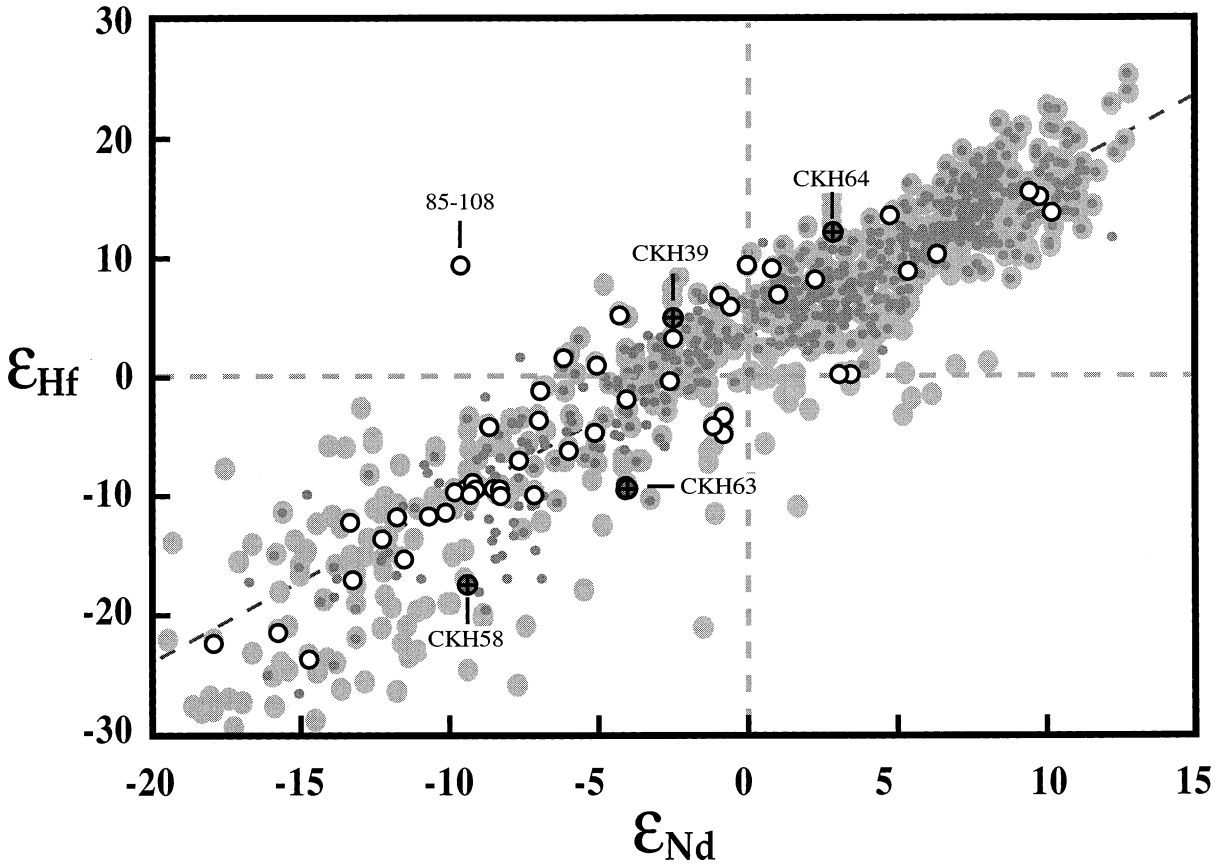


Fig. 1. Present-day Hf–Nd isotopic compositions of granulite samples (open symbols) analyzed in this study relative to the terrestrial Hf–Nd array [12]. Also shown are garnet granulites from Kilbourne Hole, New Mexico [11] (crossed circles). Most Hf–Nd data plotted here are from [12] and references therein. New data added to this diagram are from [15,16,18] and references therein.

the Sierra Madre Oriental in central Mexico (MOL-5) and from the Oaxacan complex in southern Mexico (OAX-5) [44,45]. A third sample (T-18) is a garnet-bearing metapelite xenolith occurring in a Quaternary volcanic vent (El Toro) in central Mexico. The ages of the protoliths of these lower crustal samples [46] are not well constrained but are believed to be Grenvillian (ca. 1.1–1.0 Ga). A Sm–Nd garnet whole-rock age of 0.96 Ga has been reported by Patchett and Ruiz [46] for OAX-5. Major and trace element data [45] and Nd–Sr isotopic data [44,46] for some of these and related rocks have been reported elsewhere.

### 2.5. Acatlan complex eclogites, southern Mexico

We also analyzed four samples from the Acatlan complex, a high P/T metamorphic belt in southern Mexico. These samples include three eclogites and one garnet-bearing metapelite from the Xayacatlan formation, an eclogitized sequence of the Acatlan complex. The Xayacatlan formation is interpreted to have formed from oceanic basalts and associated rocks that were tectonically emplaced adjacent to the Grenville crust of southern Mexico [47] during the Devonian. Although these and the Oaxacan complex samples are not xenoliths, they nevertheless represent an impor-

tant lithologic type that may be volumetrically important in the lower crust.

## 3. Analytical techniques

Whole-rock powders were dissolved with a HF/$HNO_3$ mixture in steel jacketed Teflon dissolution vessels for 7 days at 160°C [48]. This procedure yielded complete dissolution, with the exception of fine black graphitic particulates in a few pelitic samples. Lu–Hf elemental separations followed the procedure outlined in [13]. All samples were spiked with a mixed $^{176}Lu$–$^{180}Hf$ spike prior to chemical separation and analysis.

Lu and Hf isotopic compositions were analyzed on a VG Plasma 54 (P54) multicollector-inductively coupled plasma-mass spectrometer in Lyon, France [13,49]. Isotopic analyses on the P54 in Lyon were carried out over two 8-day periods in the Fall of 1998 and Spring of 1999. The average $^{176}Hf/^{177}Hf$ value for the JMC 475 Hf standard during these periods was $0.282161 \pm 14$ ($2\sigma$).

## 4. Results

The Hf–Nd isotopic data for the lower crustal samples are given in Table 1. Present-day isotopic values for both Hf and Nd are given with their associated in-run ($2\sigma$) errors. Also shown are the depleted mantle model Hf and Nd ages and Lu/Hf and Sm/Nd fractionation factors. The parameters used to calculate these values are given in the footnotes to Table 1.

### 4.1. Present-day Hf–Nd isotopic composition

Present-day Hf–Nd isotopic values for all xenoliths are plotted in Fig. 1 relative to the 'terrestrial array' of Vervoort and others [12] defined by Hf–Nd isotopic values from a wide variety of crust and mantle samples (3.5 Ga to the present). The terrestrial array as shown here consists of both initial (small gray circles) and present-day isotopic compositions (large gray circles): data sources of these data are given in the caption. The lower

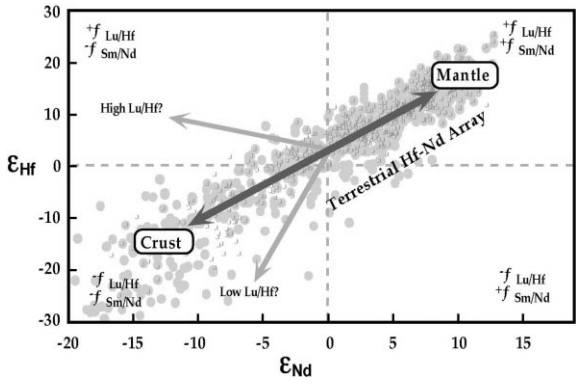


Fig. 2. Potential p/d fractionation paths for the Sm/Nd–Lu/Hf isotopic system, superimposed on the terrestrial Hf–Nd array [12]. Fractionation parallel to the terrestrial array is produced by coupled Lu/Hf and Sm/Nd fractionation with $f_{Lu/Hf}/f_{Sm/Nd}$ ratios of approximately 1.5. Large arrows show dominant fractionations in crust and mantle. Smaller arrows illustrate potential fractionation paths for sources with high and low Lu/Hf relative to Sm/Nd.

crustal samples have present-day Hf–Nd isotopic values that (1) span the entire range of the terrestrial array and (2) plot entirely within the array, with one exception (85-108).

### 4.2. Possible parent/daughter (p/d) fractionations

The mean Lu/Hf ratio of the present sample set is $0.119 \pm 3$ ($^{176}Lu/^{177}Hf = 0.0169 \pm 5$) for a mean Sm/Nd ratio of $0.247 \pm 3$ ($^{147}Sm/^{144}Nd = 0.150 \pm 2$). These values are estimated assuming a log-normal distribution and are insensitive to the exclusion of extreme values. The mean Hf/Nd ratio is $0.189 \pm 6$, identical with the bulk continental crust estimate (0.19) of Rudnick and Fountain [8] but somewhat higher than their lower crustal estimate of 0.17. Also shown in Table 1 are the p/d ratios and fractionation ($f$) values for the xenoliths, where $f_{Lu/Hf} = [(^{176}Lu/^{177}Hf_{sample})/(^{176}Lu/^{177}Hf_{CHUR}) - 1]$ and $f_{Sm/Nd} = [(^{147}Sm/^{144}Nd_{sample})/(^{147}Sm/^{144}Nd_{CHUR}) - 1]$. CHUR is the chondritic uniform reservoir reference used to approximate the bulk Earth's present-day composition. These four general groups of $f$ values (positive and negative for Lu/Hf and Sm/Nd fractionations) will give rise to coupled Hf and Nd isotopic evolution into the four quadrants of the $\varepsilon_{Hf}$–$\varepsilon_{Nd}$ plot: negative $f_{Lu/Hf}$ and $f_{Sm/Nd}$ val-

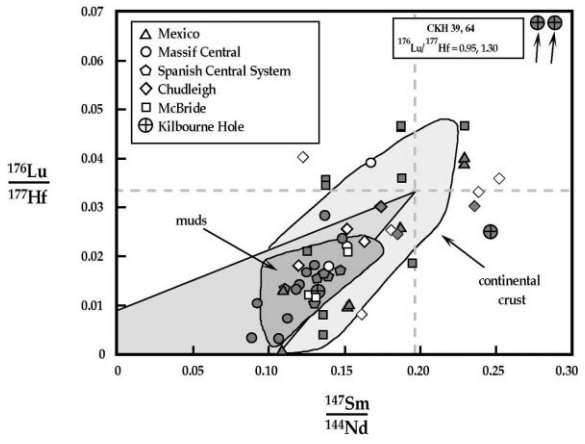


Fig. 3. Plot of $^{147}Sm/^{144}Nd$ vs. $^{176}Lu/^{177}Hf_{CHUR}$ composition of granulite samples relative to recent and ancient muds [12], and continental crust [12]. This shows to a first approximation that the fractionations of Lu/Hf and Sm/Nd in the lower crust are broadly similar to that of the upper continental crust. Gray symbols represent garnet-bearing samples; open symbols represent garnet free samples. Also shown on this diagram are four garnet granulites from Kilbourne Hole (crossed circles; data of [11]). Two samples have extremely high Lu/Hf ratios, 1–2 orders of magnitude higher than all other lower crustal samples analyzed here. Dashed lines indicate present-day $^{147}Sm/^{144}Nd$ and $^{176}Lu/^{177}Hf$ CHUR values.

ues will produce isotopic evolution toward negative $\varepsilon_{Hf}$ and $\varepsilon_{Nd}$ values and so on as illustrated in Fig. 2.

Also shown in Table 1 is $F$, the ratio of $f_{Lu/Hf}/f_{Sm/Nd}$. This is essentially a measure of the slope of the Hf–Nd evolution of each sample based on its present-day p/d ratio. Positive slopes with $F$ values of approximately 1.5 will evolve within the array. Negative slopes, due to either negative $f_{Lu/Hf}$ or $f_{Sm/Nd}$, will evolve out of the array. The rate at which a sample can evolve out of the array is a function of not only the slope of the evolution (the difference between $F$ of the sample and that of the array) but also the size of the $f_{Lu/Hf}$ and $f_{Sm/Nd}$ values. Samples with more strongly positive or negative $f$ values will evolve more quickly away from the array.

### 4.3. Lu/Hf and Sm/Nd ratios and Hf–Nd isotopic evolution

The p/d compositions of all lower crustal samples are shown in Fig. 3 relative to a compilation of crustal compositions [12]. The Hf–Nd isotopic evolution of the lower crustal samples resulting from these p/d ratios, if we assume closed system behavior, is shown in Fig. 4. Most lower crustal samples, as is the case with the vast majority of crustal samples in general, have subchondritic Sm/Nd and Lu/Hf ratios and plot in a broad band in the lower left quadrant of Fig. 3. These coherent fractionations give rise to nearly parallel Hf–Nd isotopic trends within the array (Fig. 4a). This type of Sm/Nd and Lu/Hf fractionation in crustal samples is ultimately produced by enrichment of more incompatible elements in magmas during melting processes. This is true regardless of whether the samples are mantle melts and are new to the crust (e.g. [13]), are melts of existing crust [48] or have had a long crustal history and are now part of the sedimentary record [12]. All Hf–Nd isotopic growth lines in Fig. 4a are produced by $F$ values ($f_{Lu/Hf}/f_{Sm/Nd}$) of 0.9–2.0 (delimited by the hatched wedge in the lower left quadrant of Fig. 3) and are representative of the time-integrated Lu/Hf and Sm/Nd ratios of most crustal samples.

Other samples have negative $f_{Lu/Hf}$ and $f_{Sm/Nd}$ but have slopes that cause them to diverge obliquely from the array (Fig. 4b). These have arbitrarily been distinguished from the group of samples having coherent fractionations on the basis of $F$ values $<0.9$ or $>2.0$. Only one sample from this group (RP-8 from the Massif Central) has the shallower evolution ($F<0.9$) toward the high $\varepsilon_{Hf}$ side of the array. Ten other samples (three granulites from the McBride and the Chudleigh provinces, two Mexican garnet-bearing metapelites and two Mexican eclogites) have high $F$ values and evolve toward the low $\varepsilon_{Hf}$ side of the array (Fig. 4b). All of these samples, however, have present-day $\varepsilon$ values that fall within the terrestrial array.

The opposite p/d fractionation within the terrestrial Hf–Nd array with superchondritic Sm/Nd and Lu/Hf values is shown in Fig. 3 by four samples (83-110, 83-158, M-7 and MI-6). These samples have positive $f_{Lu/Hf}$ and $f_{Sm/Nd}$ values and evolve toward positive $\varepsilon_{Hf}$ and $\varepsilon_{Nd}$ values (Fig. 4c). Although this is the dominant composition

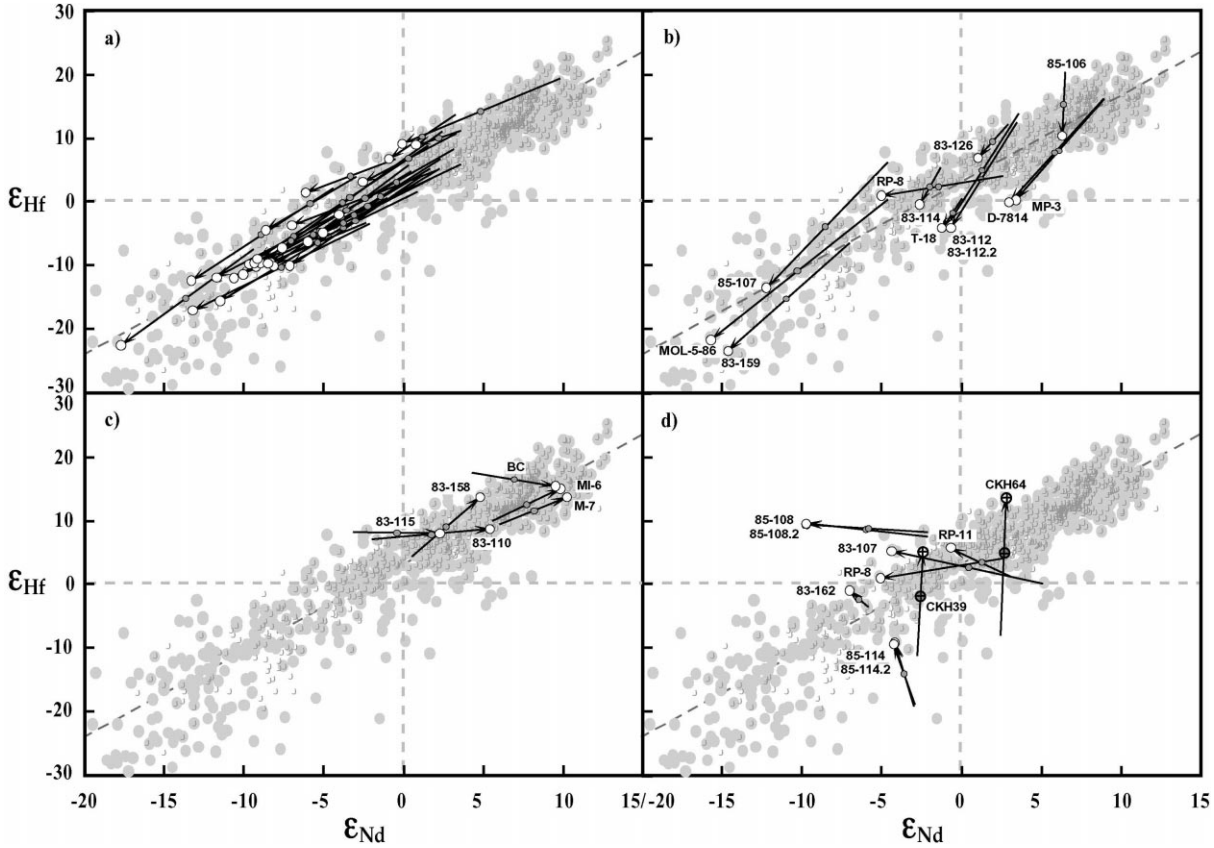


Fig. 4. Hf–Nd evolutionary paths for granulite samples based on their present-day Lu–Hf and Sm–Nd isotopic compositions. Open circles represent present-day compositions. The length of all arrows corresponds to 1 Ga of evolution assuming closed system behavior. Intermediate circles represent compositions at 0.5 Ga. Background samples of the terrestrial Hf–Nd array are the same as in Figs. 1 and 2. The crossed circles in (d) are garnet granulites from Kilbourne Hole (data of [11]). The Hf–Nd growth arrows for these two samples are only 25 Ma with intermediate points at 10 Ma. The position of the present-day compositions of these two samples still within the terrestrial Hf–Nd array in spite of the rapid radiogenic Hf growth of these samples demonstrates that the p/d ratios of these samples are recently acquired features, $<25$ Ma. See text for further description of individual panels.

and fractionation characteristic of the depleted mantle reservoir, it is rare among continental crustal samples because of the differentiation processes inherent in their formation. Most crustal samples derived from the depleted mantle have positive initial $\varepsilon_{Hf}$ and $\varepsilon_{Nd}$ values, indicative of positive time-integrated $f$ values, but present-day subchondritic p/d ratios (negative $f$ values) that now cause them to evolve toward negative $\varepsilon_{Hf}$ and $\varepsilon_{Nd}$ values. Also shown on Fig. 3 are two samples from the Chudleigh Province (83-115 and BC) that have superchondritic Sm/Nd values and near-chondritic Lu/Hf values, which cause them to evolve below the array with slightly negative $F$ trajectories (Fig. 4c).

The samples with the largest deviation from 'normal' Lu/Hf and Sm/Nd fractionations and thus with the greatest potential for evolving to Hf and Nd compositions out of the terrestrial array are those with superchondritic Lu/Hf and sub- or near-chondritic Sm/Nd (Fig. 4d). There are five examples of these: one each from the French Massif Central (RP-11) and Chudleigh Province (83-107) and three from the McBride Province (83-162, 85-114 and 85-108). Although all these samples have trajectories that will evolve

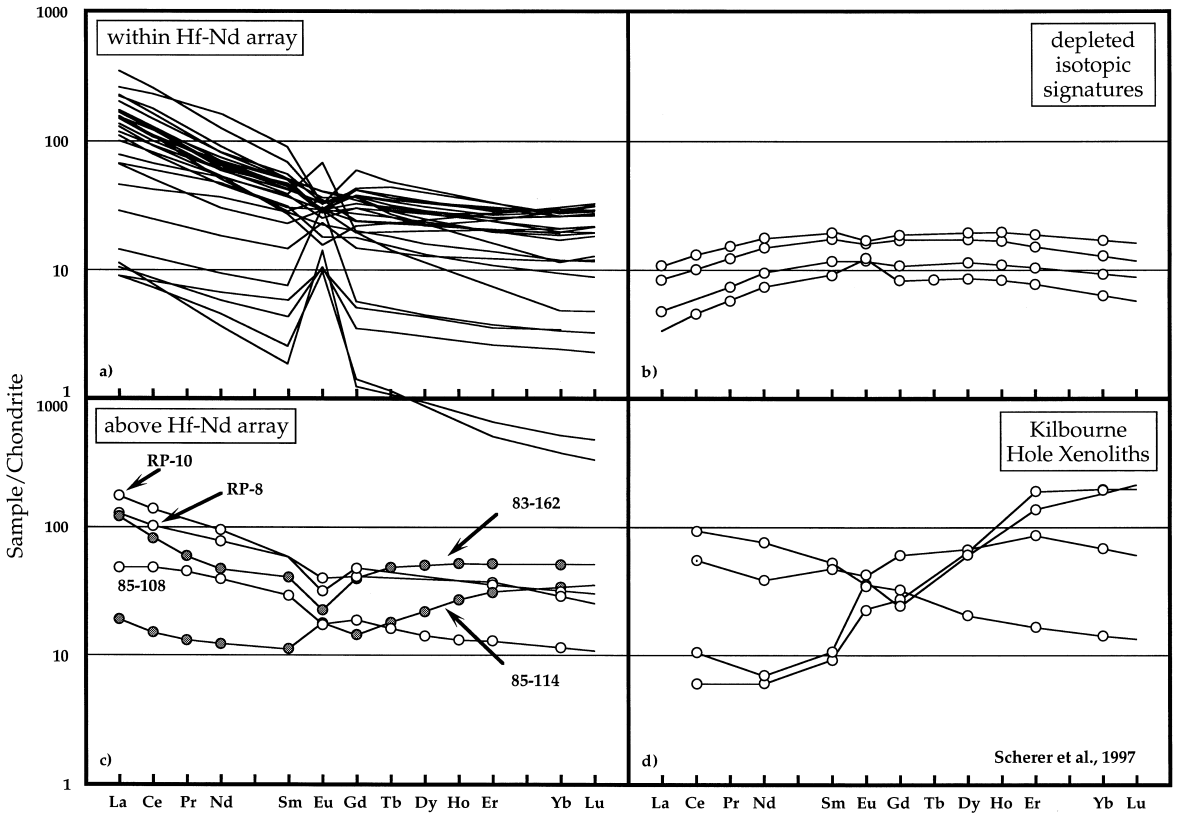


Fig. 5. Chondrite-normalized REE patterns of granulite samples: (a) samples with Hf–Nd evolution within array (Fig. 4a); (b) samples with ${}^{+}f_{Lu/Hf}$ and ${}^{+}f_{Sm/Nd}$ values (Fig. 4c); (c) samples evolving to compositions above terrestrial array (Fig. 4d); (d) Kilbourne Hole garnet granulite samples [11] (Fig. 4d). Other REE data are from [23,29,34,35,45]. Hf generally behaves similar to LREEs in terms of partitioning between melts and solids appropriate to this study. The two xenoliths from this study that do show a modest garnet effect (83-162 and 85-114) are shown in Fig. 4d by the shaded circles.

toward anomalous Hf–Nd isotopic compositions, with one exception (85-108), all have present-day isotopic compositions that are within the array (Fig. 4d).

## 5. Discussion

### 5.1. Residual garnet and high Lu/Hf reservoirs in the lower crust?

Anomalously high Lu/Hf ratios in a source region can be the result of two primary processes: melt extraction in the presence of garnet to produce higher Lu/Hf in a restite, or crystallization of garnet from a magma, resulting in high Lu/Hf in a cumulate. Both scenarios involve the role of garnet, which has a high partition coefficient for heavy rare-Earth elements and results in the preferential retention of Lu over Hf. Residual garnet will thus have high Lu/Hf that will evolve to highly radiogenic Hf isotope compositions over time [48,50]. However, if the garnet in these samples is instead a metamorphic phase, then enrichment of Lu/Hf will not occur, and we would not expect production of radiogenic Hf.

The latter appears to be the case for most of the lower crustal samples analyzed in this study. Although more than three-fourths of the samples are garnet-bearing, there is scant evidence that the

garnet in these samples is a residual phase from a prior melting event (Fig. 3). Garnet-bearing samples exhibit the same range in p/d ratios as continental crust. There is no correlation between garnet-bearing samples and elevated Lu/Hf ratios.

In a study of lower crustal granulite xenoliths from Kilbourne Hole, New Mexico, Scherer and others [11] found extremely high Lu concentrations (7–8 ppm) and Lu/Hf ratios ($^{176}Lu/^{177}Hf$ of 0.93 and 1.30) in two garnet-bearing granulite xenoliths, which clearly reflect preferential partitioning of Lu over Hf in garnet (Fig. 3). These xenoliths also have slightly superchondritic Sm/Nd ratios ($^{147}Sm/^{144}Nd$ of 0.297 and 0.301). The extreme elevation of Lu/Hf in these samples relative to all the lower crustal samples analyzed in the present study (Fig. 3) results in steep and rapid production of radiogenic Hf: Hf evolves by 64 and 86 $\varepsilon_{Hf}$ units in 100 million years, with only negligible Nd growth ($\sim 1$ $\varepsilon_{Nd}$ unit) over the same time. This rapid radiogenic Hf growth is plotted in Fig. 4d for the Kilbourne Hole samples (CKH39 and CKH64). Note that, in contrast to the growth trajectories for all the other samples whose total length corresponds to 1.0 Ga (with intermediate marks at 0.5 Ga), the growth lines illustrated for the KBH samples represent only 25 Ma, with intermediate marks at 10 Ma. (Fig. 4d). These isotope systematics in the Kilbourne Hole samples suggest that garnet formed as a residual phase during early magmatic processes ($< 25$ Ma) in the Rio Grande Rift [11]. Clearly, if a source such as this was volumetrically significant in the lower crust and was allowed to evolve for hundreds of millions of years, it would be easily recognizable by its Hf isotopic signature.

How volumetrically important might such lithologies be? The widespread occurrence of a high Lu/Hf reservoir in the deep crust was what Vervoort and Patchett [48] searched for in a variety of Precambrian granites derived by melting of pre-existing ($> 300$ Ma older) crust. All of these samples, however, had Hf and Nd isotopic compositions that plotted within the terrestrial array. Vervoort and Patchett [48] concluded that either garnet is not a widespread residual phase in the mid to lower crust, or that such high Lu/Hf garnet-bearing assemblages do not contribute to magmas originating from or passing through the mid to lower crust [48].

Lower crustal samples from our study that are most likely to exhibit a radiogenic Hf garnet effect are those with $^{176}Lu/^{177}Hf$ ratios higher than chondritic (i.e. positive $f_{Lu/Hf}$ values). Of these, six also have positive $f_{Sm/Nd}$ values (Fig. 4c) and of the five samples with $^{+}f_{Lu/Hf}$ and $^{-}f_{Sm/Nd}$ values (Fig. 4d), three (RP-11, 83-107 and 85-108) have superchondritic Lu/Hf ratios due to mainly low Hf concentrations (all = 1.2 ppm), rather than elevated Lu contents (all = 0.3 ppm Lu; Table 1). Two McBride Province samples (83-162 and 85-114) have modal garnet [35] and do show a modest garnet effect. These samples have relatively high Lu concentrations ($\sim 1$ ppm) which result in elevated Lu/Hf ratios (0.036 and 0.046). These Lu/Hf ratios, however, are still only slightly superchondritic and are quite modest compared to the two Kilbourne Hole garnet granulites [11].

The Lu–Hf and Sm–Nd systematics of these samples are reflected in their REE patterns. Most granulite xenoliths (Fig. 5a) have broadly similar REE patterns with LREE enrichment, Eu anomalies (both positive and negative) and flat to HREE-depleted patterns. All of the samples in Fig. 5a have Hf and Nd isotopic compositions that plot within the array. In contrast, the Kilbourne Hole garnet granulites with high Lu/Hf ratios have pronounced LREE depletion and HREE enrichment, characteristic of residual garnet (Fig. 5d). The two McBride samples with a modest garnet effect (83-162 and 85-114) have flat to slightly enriched HREE, but with much lower abundance of HREE than the Kilbourne Hole garnet granulites. Considering the lack of evidence for residual garnet in the samples in this study, it is not surprising that these lower crustal samples show no diversion from the terrestrial Hf–Nd array.

The samples in this study were not selected to search for a radiogenic Hf garnet effect but rather to give a first-order view of Hf–Nd isotopic systematics of the lower crust from well characterized suites of samples. Based on this initial survey, residual garnet-bearing assemblages with high time-integrated Lu/Hf ratios do not seem to be a widespread feature of the lower crust. Although

most of the samples analyzed here are garnet-bearing, it is clear that most of this garnet is not a residual phase. Of the 50 samples we have analyzed, only two samples exhibit a modest garnet effect and even in these samples the radiogenic Hf growth is rather slow and has been insufficient for the samples to evolve out of the terrestrial Hf–Nd array.

### 5.2. Coherent Hf–Nd behavior in the silicate Earth

There are three main observations that can be made about the Hf–Nd data of the lower crustal xenoliths we have examined in this paper. First, the lower crustal samples span a wide range of Hf–Nd isotopic compositions that mirror the terrestrial array. It appears, therefore, that we have sampled a representative range of Hf–Nd isotopic compositions and p/d ratios in the lower crust. Second, these samples have a wide variety of p/d ratios, which have produced Hf–Nd isotopic evolutionary paths in many divergent directions. The majority of these samples, however, have isotopic growth that tracks along the terrestrial Hf–Nd array. Third, in spite of this range of fractionations and evolutionary trajectories, all granulite samples, with one exception, have evolved to present-day isotopic compositions within the terrestrial array. Thus the lower crust appears to be broadly similar to upper crustal samples in terms of overall Hf–Nd isotopic composition and evolution. We do not imply that there are no reservoirs with distinctive Hf–Nd isotopic compositions. Indeed, ferromanganese crusts are demonstrably radiogenic in Hf and plot along a trend at an oblique angle to the Hf–Nd array [51]. Other reservoirs (e.g. lithospheric mantle [52]; 1.4 Ga anorogenic granites [50]) are suggested to have Hf–Nd isotopic compositions distinct from the mantle OIB array. What we do imply is that, to a first order, the upper and lower crustal reservoirs are similar.

This first-order coherency of Hf–Nd isotopes and parallel Lu/Hf and Sm/Nd fractionations in the crust and mantle is a surprising outcome of recent Hf–Nd isotopic investigations of various terrestrial reservoirs [12]. This contrasts markedly with the Hf–Nd isotopic evolution of lunar [53,54] and Martian [55] samples which record highly divergent Lu/Hf and Sm/Nd fractionations after the primary differentiation of these bodies. None of the minerals that account for substantial fractionation of Sm/Nd and Lu/Hf seems to achieve Hf–Nd decoupling in the terrestrial system. The overall crust–mantle coherency in the terrestrial Hf–Nd array also seems to reflect efficient mixing processes of a dynamic Earth: mantle convection, homogenization in the crust via sedimentary processes, and recycling of crustal materials back into the mantle [12].

Within the lower crust, there seems to be a range of p/d fractionations capable of producing divergent Hf–Nd evolution. The reason these do not result in significant isotopic divergence from the terrestrial array may simply be due to the recent timing of these p/d fractionations and/or the scale of lower crustal heterogeneities.

A striking example of a young fractionation event is in the contrast between the extreme $^{176}Lu/^{177}Hf$ ratios in the Kilbourne Hole garnet granulites and their rather normal $^{176}Hf/^{177}Hf$ ratios. In the Kilbourne Hole case, this inconsistency is explained if their elevated Lu/Hf ratios were produced by very recent fractionation ($<25$ Ma [11]). This age corresponds to the initiation of mafic magmatism of the Rio Grande Rift but is much younger than the protolith age (ca. 1.6 Ga [56]) of most lower crustal xenoliths in that region.

Perhaps the most significant reason we do not see large Hf–Nd isotopic divergence from the mantle array is due to the size of the xenoliths relative to lower crustal heterogeneity. Most xenoliths are small compared to the compositional layering often present in these samples and are certainly much smaller than the heterogeneity believed to exist in the lower crust. Therefore, some of the divergence seen in coupled Hf–Nd evolution (e.g. Fig. 4b,d) may reflect p/d fractionations and elemental variations that exist on the scale of small xenolith samples, but not on a larger (reservoir) scale.

Some of the interest in the Hf–Nd isotopic composition of the lower crust has been in its relationship to the upper crust, mantle and the BSE reference. Blichert-Toft and Albarède [21]

have argued that the BSE lies significantly below the terrestrial array and hypothesized the existence of a hidden reservoir in the Earth needed to balance terrestrial compositions. Others [12,57] have argued that the mismatch between BSE and the terrestrial array may be an artifact due to the uncertainty in the Lu–Hf and Sm–Nd chondritic reference points.

Our data suggest that the lower crust is similar to the upper crust in terms of both its present-day p/d values (Fig. 3), Hf/Nd ratios, and time-integrated Lu–Hf and Sm–Nd evolution (Fig. 4). We have examined only a few xenolith suites in the present paper and these may not be representative of the entire lower crust. However, the lack of significant HREE enrichment in the vast majority of lower crustal xenoliths [58] suggests that our findings are globally relevant. As a whole, the lower crust does not appear to be a reservoir with a unique Hf–Nd composition. Thus, as is true for Sm/Nd, Lu/Hf ratios are not greatly fractionated by lower crustal processes and the lower crust does not appear to be a reservoir with a long-lived isotopic history distinct from the upper crust.

In closing, we offer the caveat that the xenoliths we have examined are all from post-Archean terranes and it is possible that the Hf isotopic composition of the lower crust and its formation in the Archean is fundamentally distinct from the post-Archean. Evidence for this comes from the occurrence of TTG (Trondhjemite–Tonalite–Granodiorite association) magmas in the Archean. The TTGs are characteristically depleted in HREEs, indicative of residual garnet in their sources. It is possible that these magmas and their source regions will evolve to compositions below and above the Hf–Nd terrestrial array, respectively. To our knowledge, there have been no Hf isotope analyses of TTG samples that have a strong HREE-depleted character. Nevertheless, we have not observed anomalous Hf isotopic compositions, either initial or present-day, in any of the Archean samples examined thus far including Archean juvenile (mantle-derived) samples [13], Archean shales [12], Archean komatiites [16,17] and Precambrian granitoids melted from Archean crust [48].

## Acknowledgements

We are grateful to Philippe Télouk for his expertise in maintaining the P54 in top running condition and Joaquin Ruiz and Diana Meza-Figueroa for providing the Mexican samples. We thank Chris Hawkesworth, Clark Johnson and Vincent Salters for their constructive and helpful reviews. This research was funded by NSF Grants EAR-9526536 and EAR-9814885 and by the Program Dynamique des Transports Terrestres of Institut National des Sciences de l'Univers for the analytical work at the Ecole Normale Supérieure de Lyon. NSF supplemented EAR-9526536, and enabled this collaboration between the University of Arizona and Lyon.*[AH]*

## References

[1] R.L. Rudnick, Xenoliths – Samples of the lower continental crust, in: D.M. Fountain, R. Arculus and R.W. Kay (Eds.), Continental Lower Crust, Elsevier, Amsterdam, 1992, pp. 269–316.
[2] R.L. Rudnick and T. Presper, Geochemistry of intermediate- to high-pressure granulites, in: D. Vielzeuf and P. Vidal (Eds.), Granulites and Crustal Evolution, NATO ASI Series, Kluwer, Dordrecht, 1990, pp. 523–550.
[3] S.R. Bohlen, K. Mezger, Origin of granulite terranes and the formation of the lowermost continental crust, Science 244 (1989) 326–329.
[4] S.R. Bohlen, On the formation of granulites, J. Metamorph. Geol. 9 (1991) 223–229.
[5] K. Mezger, Temporal evolution of regional granulite terranes: Implications for the formation of lowermost continental crust, in: D.M. Fountain, R. Arculus and R.W. Kay (Eds.), Continental Lower Crust, Elsevier Science, New York, 1992, pp. 447–478.
[6] W.S. Holbrook, W.D. Mooney and N.I. Christensen, The seismic velocity structure of the deep continental crust, in: D.M. Fountain, R. Arculus and R.W. Kay (Eds.), Continental Lower Crust, Elsevier Science, New York, 1992, pp. 1–44.
[7] N.I. Christensen, W.D. Mooney, Seismic velocity structure and composition of the continental crust: A global view, J. Geophys. Res. 100 (1995) 9761–9788.
[8] R.L. Rudnick, D.M. Fountain, Nature and composition of the continental crust: a lower crustal perspective, Rev. Geophys. 33 (1995) 267–309.
[9] T. Rushmer, Experimental high-pressure granulites: Some applications to natural mafic xenolith suites and Archean granulite terranes, Geology 21 (1993) 411–414.
[10] D. Vielzeuf, J.R. Holloway, Experimental determination

of the fluid-absent melting relations in the pelitic system: consequences for crustal differentiation, Contrib. Mineral. Petrol. 98 (1988) 257–276.
[11] E.E. Scherer, K.L. Cameron, C.M. Johnson, B.L. Beard, K.M. Barovich, K.D. Collerson, Lu–Hf geochronology applied to dating Cenozoic events affecting lower crustal xenoliths from Kilbourne Hole, New Mexico, Chem. Geol. 142 (1997) 63–78.
[12] J.D. Vervoort, J. Blichert-Toft, P.J. Patchett, F. Albarède, Relationships between Lu–Hf and Sm–Nd isotopic systems in the global sedimentary system, Earth Planet. Sci. Lett. 168 (1999) 79–99.
[13] J.D. Vervoort, J. Blichert-Toft, Evolution of the depleted mantle: Hf isotope evidence from juvenile rocks through time, Geochim. Cosmochim. Acta 63 (1999) 533–556.
[14] J. Blichert-Toft, F. Albarède, Hf isotopic compositions of the Hawaii Scientific Drilling Project core and the source mineralogy of Hawaiian basalts, Geophys. Res. Lett. 26 (1999) 935–938.
[15] J. Blichert-Toft, F.A. Frey, F. Albarède, Hf isotope evidence for pelagic sediments in the source of Hawaiian basalts, Science 285 (1999) 879–882.
[16] J. Blichert-Toft, N.T. Arndt, Hf isotopic composition of komatiites, Earth Planet. Sci. Lett. 171 (1999) 439–451.
[17] J. Blichert-Toft, F. Albarède, R. Frei, D. Bridgwater, The Nd and Hf isotopic evolution of the mantle through the Archean. Results from the Isua supracrustals, West Greenland, and from the Birimian terranes of West Africa, Geochim. Cosmochim. Acta 63 (1999) 3901–3914.
[18] A. Stracke, V. Salters and K.W.W. Sims, Assessing the Presence of Garnet-Pyroxenite in the Mantle Sources of Basalts Through Combined Hafnium–Neodymium–Thorium Isotope Systematics, Geochemistry, Geophysics, Geosystems 1 (Paper 1999GC000013), 2000.
[19] S.B. Jacobsen, G.J. Wasserburg, Sm–Nd isotopic evolution of chondrites, Earth Planet. Sci. Lett. 50 (1980) 139–155.
[20] S.B. Jacobsen, G.L. Wasserburg, Sm–Nd isotopic evolution of chondrites and achondrites, II, Earth Planet. Sci. Lett. 67 (1984) 137–150.
[21] J. Blichert-Toft, F. Albarède, The Lu–Hf isotope geochemistry of chondrites and the evolution of the mantle-crust system, Earth Planet. Sci. Lett. 148 (1997) 243–258.
[22] A. Leyreloup, C. Dupuy, R. Andriambololona, Catazonal xenoliths in French Neogene volcanic rocks: constitution of the lower crust. 2. Chemical composition and consequences of the evolution of the French Massif Central Precambrian crust, Contrib. Mineral. Petrol. 62 (1977) 283–300.
[23] H. Downes, C. Dupuy, A.F. Leyreloup, Crustal evolution of the Hercynian belt of western Europe: evidence from lower crustal granulitic xenoliths (French Massif Central), Chem. Geol. 83 (1990) 209–231.
[24] C. Dupuy, A. Leyreloup, J. Vernieres, The lower continental crust of the Massif Central (Bournac, France) - with special references to REE, U and Th composition, evolution, heat-flow production, Phys. Chem. Earth 11 (1977) 401–416.
[25] J. Dostal, C. Dupuy, A. Leyreloup, Geochemistry and petrology of meta-igneous granulitic xenoliths in Neogene volcanic rocks of the Massif Central, France – implications for the lower crust, Earth Planet. Sci. Lett. 50 (1980) 31–40.
[26] H. Downes, P.D. Kempton, D. Briot, R.S. Harmon, A.F. Leyreloup, Pb and O isotope systematics in granulite facies xenoliths, French Massif Central: implications for crustal processes, Earth Planet. Sci. Lett. 102 (1991) 342–357.
[27] S. Costa, P. Rey, W. Todt, Late Carboniferous age of lower-crustal granulite-facies xenoliths in the eastern French Massif Central: Implications for post-thickening crustal processes, Terra Nova 5 (1993) 233.
[28] H. Downes, J.-L. Duthou, Isotopic and trace-element arguments for the lower-crustal origin of Hercynian granitoids and Pre-Hercynian orthogneisses, Massif Central (France), Chem. Geol. 68 (1988) 291–308.
[29] C. Villaseca, H. Downes, C. Pin, L. Barbero, Nature and composition of the lower continental crust in central Spain and the granulite-granite linkage: inferences from granulitic xenoliths, J. Petrol. 40 (1999) 1465–1496.
[30] L.J.G. Schermerhorn, H.N.A. Priem, N.A.I.M. Bjoelrijk, E.H. Hebeda, E.A.T. Verdurmen, R.H. Verschure, Age and origin of the Messejana dolerite fault-dike system (Portugal and Spain) in the light of the opening of the North Atlantic Ocean, J. Geol. 86 (1978) 299–309.
[31] C. Villaseca, L. Barbero, G. Rogers, Crustal origin of Hercynian peraluminous granitic batholiths of Central Spain: petrological, geochmical and isotopic (Sr, Nd) constraints, Lithos 43 (1998) 55–79.
[32] R.W. Johnson, Intraplate Volcanism in Eastern Australia and New Zealand, Cambridge Univ. Press, Canberra, 1989, pp. 408.
[33] L.P. Black, T.H. Bell, M.J. Rubenach, I.W. Withnall, Geochronology of discrete structural-metamorphic events in a multiply deformed Precambrian terrain, Tectonophysics 54 (1979) 103–137.
[34] R.L. Rudnick, W.F. McDonough, M.T. McCulloch, S.R. Taylor, Lower crustal xenoliths from Queensland, Australia: evidence for deep crustal assimilation and fractionation of continental basalts, Geochim. Cosmochim. Acta 50 (1986) 1099–1115.
[35] R.L. Rudnick, S.R. Taylor, The composition and petrogenesis of the lower crust: a xenolith study, J. Geophys. Res. 92 (1987) 13981–14005.
[36] R.L. Rudnick, I.S. Williams, Dating the lower crust by ion microprobe, Earth Planet. Sci. Lett. 85 (1987) 145–161.
[37] A.E. Saal, R.L. Rudnick, G.E. Ravizza, S.R. Hart, Re–Os isotope evidence for the composition, formation and age of the lower continental crust, Nature 393 (1998) 58–61.
[38] S.M. Kay, R.W. Kay, Thermal history of the deep crust inferred from granulite xenoliths, Queensland, Australia, Am. J. Sci. 283-A (1983) 486–513.

[39] R.L. Rudnick and S.R. Taylor, Petrology and geochemistry of lower crustal xenoliths from northern Queensland and inferences on lower crustal composition, in: B. Drummond (Ed.), The Australian Lithosphere, Spec. Publ. 17, Geol. Soc. Austr., Canberra, 1991, pp. 198–208.
[40] R.L. Rudnick, Nd and Sr isotopic compositions of lower crustal xenoliths from North Queensland, Australia: implications for Nd model ages and crustal growth processes, Chem. Geol. 83 (1990) 195–208.
[41] P.D. Kempton, R.S. Harmon, Oxygen-isotope evidence for large-scale hybridization of the lower crust during magmatic underplating, Geochim. Cosmochim. Acta 55 (1992) 971–986.
[42] R.L. Rudnick, S.L. Goldstein, The Pb isotopic compositions of lower crustal xenoliths and the evolution of lower crustal Pb, Earth Planet. Sci. Lett. 98 (1990) 192–207.
[43] F. Ortega-Gutierrez, Metamorphic belts of southern Mexico and their tectonic significance, Geofis. Int. 20 (1981) 177–202.
[44] J. Ruiz, P.J. Patchett, F. Ortega-Gutierrez, Proterozoic and Phanerozoic basement terrances of Mexico from Nd isotope studies, Geol. Soc. Bull. Am. 100 (1988) 274–281.
[45] S.J. Roberts, J. Ruiz, Geochemistry of exposed granulite facies terrains and lower crustal xenoliths in Mexico, J. Geophys. Res. 94 (1989) 7961–7974.
[46] P.J. Patchett, J. Ruiz, Nd isotopic ages of crust formation and metamorphism in the Precambrian of eastern and southern Mexico, Contrib. Mineral. Petrol. 96 (1987) 523–528.
[47] D.M. Meza-Figueroa, Geochemistry and characterization of intermediate temperature eclogites from the Acatlan complex, southern Mexco, unpubl. Ph.D. Thesis, Univ. of Arizona, 1998.
[48] J.D. Vervoort, P.J. Patchett, Behavior of hafnium and neodymium isotopes in the crust: Constraints from Precambrian crustally derived granites, Geochim. Cosmochim. Acta 60 (1996) 3717–3733.
[49] J. Blichert-Toft, C. Chauvel, F. Albarède, Separation of Hf and Lu for high precision isotope analysis of rock samples by magnetic sector-multiple collector ICP-MS, Contrib. Mineral. Petrol. 127 (1997) 248–260.
[50] C.M. Johnson, S.B. Shirey, K.M. Barovich, New approaches to crustal evolution studies and the origin of granitic rocks: what can the Lu–Hf and Re–Os isotope systems tell us?, Trans. R. Soc. Edinb. 87 (1996) 339–352.
[51] F. Albarède, T. Simonetti, J.D. Vervoort, J. Blichert-Toft, W. Abouchami, A Hf–Nd isotopic correlation in ferromanganese nodules, Geophys. Res. Lett. 25 (1998) 3895–3898.
[52] B.L. Beard, C.M. Johnson, Hafnium isotope evidence for the origin of Cenozoic basaltic lavas from the southwestern United States, J. Geophys. Res. 102 (1997) 20149–20178.
[53] D.M. Unruh, P. Stille, P.J. Patchett, M. Tatsumoto, Lu–Hf and Sm–Nd evolution in Lunar mare basalts, J. Geophys. Res. 89 (Suppl.) (1984) B459–B477.
[54] B.L. Beard, L.A. Taylor, E.E. Scherer, C.M. Johnson, G.A. Snyder, The source region and melting mineralogy of high-titanium and low-titanium lunar basalts deduced from Lu–Hf isotope data, Geochim. Cosmochim. Acta 62 (1998) 525–544.
[55] J. Blichert-Toft, J.D. Gleason, P. Télouk, F. Albarède, The Lu–Hf isotope geochemistry of shergottites and the evolution of the Martian mantle-crust system, Earth Planet. Sci. Lett. 173 (1999) 25–39.
[56] E.R. Padovani and M.R. Reid, Field guide to Kilbourne Hole maar, Dona Ana County, New Mexico, in: C.E. Chapin and J. Zicek (Eds.), Field Excursions to Volcanic Terranes in the Western United States, Vol. I: Southern Rocky Mountain Region, New Mex. Bur. Mines Min. Res., Mem. 46, 1989, pp. 174–179.
[57] V.J.M. Salters, W.M. White, Hf isotope constraints on mantle evolution, Chem. Geol. 145 (1998) 447–460.
[58] GERM, Geochemical Earth Reference Model, http://www.earthref.org/germ/, 2000.